

Turbidity Currents

Dr. Rajashree Lodh

BE (Civil) (TIT, Tripura), ME (Civil) (BESU, Shibpur), PhD (Civil) (IIT Kharagpur)
Assistant Professor, Heritage Institute of Technology, Kolkata, West Bengal, INDIA, and
Post-doctoral Researcher,
MultiSpectra Consultants,
23, Biplabi Ambika Chakraborty Sarani,
Kolkata – 700029, West Bengal, INDIA.
E-mail: shree1504@gmail.com

Dr. Amartya Kumar Bhattacharya

BCE (Hons.) (Jadavpur), MTech (Civil) (IIT Kharagpur), PhD (Civil) (IIT Kharagpur),
Cert.MTERM (AIT Bangkok), CEng(I), FIE, FACCE(I), FISH, FIWRS, FIPHE, FIAH, FAE,
MIGS, MIGS – Kolkata Chapter, MIGS – Chennai Chapter, MISTE, MAHI, MISCA, MIAHS,
MISTAM, MNSFMFP, MIIBE, MICI, MIEES, MCITP, MISRS, MISRMTT, MAGGS, MCSI,
MIAENG, MMBSI, MBMSM
Chairman and Managing Director,
MultiSpectra Consultants,
23, Biplabi Ambika Chakraborty Sarani,
Kolkata – 700029, West Bengal, INDIA.
E-mail: dramartyakumar@gmail.com

CONTENTS

1 Introduction

1.1 General

1. Scope of this Work

2

References

2 Turbidity Currents

2. General

1

2. Review of Literature

2

2. Velocity Distribution

3

2. Concentration Distribution

4

2. Conclusion

5

References

1

Introduction

1.1 General

India's water resources become increasingly strained, as the population of India continues to expand. Discharge of untreated sewage is the single most important cause for pollution of surface and ground water in India. Heavy pollution from open sewers is common place in urban areas and arsenic contamination of groundwater continues to threaten the health and well-being of local communities. India is defined as a 'water stressed' country and innovative methods to provide cost-effective water treatment to communities are a crucial requirement if growing populations are to be sustainable. Sewage are to be removed by applying different sewage treatments. A natural river continually picks up waste products from and drops them on its bed throughout its course. Knowledge of sediment transport can be applied extensively in civil engineering such as to plan how to control the flow of water in culverts, over spillways, below pipelines and around bridge piers and abutments, excess of which can damage the environment and failure of foundation of the structures. Moreover, when suspended load of sediment is substantial due to human activities, it can cause environmental hazards including filling up of the channels by siltation. Sediment transport is the movement of organic and inorganic particles by water. In general, the greater the flow, the more sediment will be conveyed. Water flow can be strong enough to suspend particles in the water column as they move downstream, or simply push them along the bottom of a waterway. Transported sediment may include mineral matter, chemicals and pollutants, and organic material. The total load includes all particles moving as bed load, suspended load, and wash load.

Turbidity, as an optical property of water, is one of the more difficult parameters to measure. Turbidity is caused by particles and coloured material in water. Total suspended solids (TSS) are the main cause of turbidity. Turbidity currents are most typically underwater currents of usually rapidly moving, sediment-laden water

moving down a slope. Turbidity currents can also occur in other fluids besides water. In the most typical case of oceanic turbidity currents, sediment laden waters situated over sloping ground flow down-hill because they have a higher density than the adjacent waters. The driving force behind a turbidity current is gravity acting on the high density of the sediments temporarily suspended within a fluid. As such currents flow, they often have a "snow-balling-effect", as they stir up the ground over which they flow, and gather even more sedimentary particles in their current. Their passage leaves the ground scoured and eroded. Once a turbidity current reaches the calmer waters of the flatter area, the particles borne by the current settle out of the water column. The sedimentary deposit of a turbidity current is called a turbidite. When sediment transport removes material from a streambed or bank, the erosion process is called scour. Scour can occur anywhere where there is water flow and erodible material. Local scour is an engineering term for the isolated removal of sediment at one location, such as the base of underwater structures, including bridge piers and abutments. This localized erosion can cause structural failure, as bridges and overwater constructions rely on the bed sediment to support them.

1.2 Scope of this work

The objective of the present work is to understand the hydrodynamics of turbidity currents over plane beds based on velocity and concentration distributions. The sewage can be removed by offset jets.

References

- Dey, S. (2014). *Fluvial Hydrodynamics: Hydrodynamic and Sediment Transport Phenomena*, Springer, Berlin.
- Metcalf, L., Eddy, H. P. (1922). *Sewerage and Sewage Disposal: A Textbook*. New York: McGraw-Hill.

2

Turbidity Currents

2.1 General

Turbidity currents are density currents that are generated due to the density difference of suspended sediments and water in a mixture. In turbidity currents, suspended sediment makes the density of the mixture greater than the density of the ambient water and provides the driving force; the sediment laden flow must generate enough turbulence to hold the sediment in suspension. They can be observed in the flows entering large bodies of water containing high concentration of suspended sediments. These are sediment-laden gravity currents that exchange sediment with the bed by erosion or deposition as the flow travels over the down slope. Turbidity currents derive this driving force from the sediment in suspension. They experience a resisting shear force on the bed and entrain water from above. Two types of turbidity currents can be distinguished: Low velocity, low density and high velocity, high density. High velocity, high density turbidity currents often carry suspended materials introduced near the shore to the deep sea.

Turbidity currents can be originated by various processes. Discharges of large amounts of sediments, e.g., mine tailings, underwater landslides caused by earthquakes, and re-suspension of suspended materials by waves during storms are three possibilities. Turbidity currents can be eroding or depositing, accelerating or decelerating, depending on the combination of initial conditions, bed slope, and size of sediment particles. A turbidity current with deposition and erosion is a flow in three components: clear ambient water, turbid water and sediment (bed material). The turbidity current entrains clear water into the flow and simultaneously either deposits suspended sediment on the channel bed, or entrains bed material into the flow. Actually turbidity current entrains and deposits at the same time, but there is a net flux either to the bed (depositing current) or from the bed (entraining current). Turbidity currents are self-generated currents. The flow will vanish when

all suspended materials are deposited on the bottom, and grow when sediments are entrained from the bed.

Turbidity current is made up of a front or head advancing into the ambient fluid, being followed by the body. The driving force for the front (unsteady flow) is the pressure gradient which is due to the density difference between the front and the ambient fluid. The driving force for body (steady flow) is the gravitational force of the heavier fluid. A schematic diagram of turbidity current is shown in Fig. 2.1.

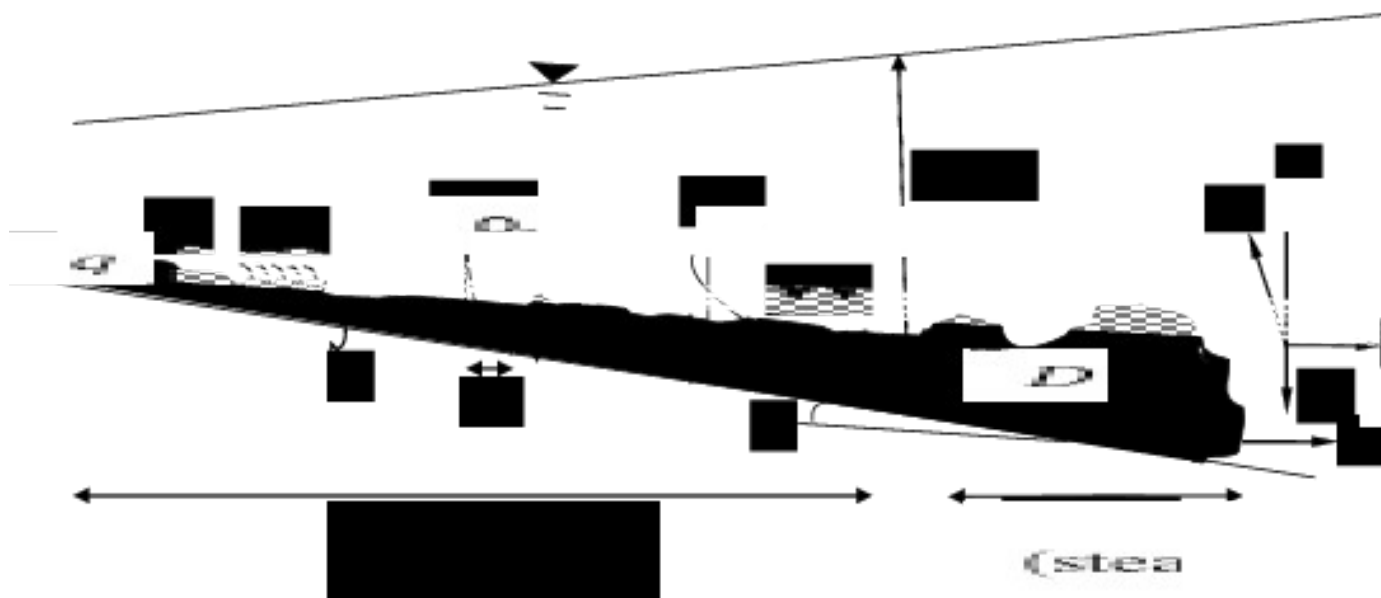


Fig. 2.1 Definition sketch of turbidity current

2.2 Review of Literature

The characteristics and behaviour of turbidity currents was studied by many investigators and some of them are reviewed below.

Akiyama and Stefan (1985) derived various equations that govern the movement of two-dimensional gradually varied turbidity currents in reservoirs and over beaches and solved numerically. The model included and quantified all mechanisms which control accelerating and decelerating turbidity currents. The model consisted of depth-integrated equations for conservation of mass and volume, momentum equations and an empirical relationship for water entrainment and sediment entrainment. The equations were numerically solved by a Runge-Kutta method. The flow of turbidity current was found to be dependent on three factors: initial conditions, the size of the suspended sediment particles and the channel slope. The model explained clearly the differences as well as the similarities between subsurface gravity currents with and without sediment erosion and deposition. Parker et al. (1986) presented a general concept of the equations of motion of turbidity currents, their closure, and their solution for the continuous, spatially developing case in submarine canyons. Special attention is drawn on the possibility of self-acceleration, or ignition, by means of the incorporation of bed sediment into the current. Two models are presented. The first of these is the three-equation model, which can be considered as a generalization of the model of Ellison and Turner (1959) for simple, conservative density currents to the case of eroding and depositing turbidity currents. The self-acceleration predicted by the three-equation model was so strong that the energy constraint failed to be satisfied. The problem was rectified by the formulation of a four-equation model, in which an explicit accounting was made of the mean energy of the turbulence. Sediment entrainment from the bed was linked to the level of turbulence in the four-equation model. Parker et al. (1987) conducted various experiments to determine the behaviour of turbidity currents laden with non-cohesive silt (silica flour) moving down a slope the bed of which was covered with similar silt. The motion of the head was not studied; measurements were concentrated on the continuous part of the current that was essentially constant in time but developing in space. Only supercritical currents were studied. The currents were free to erode sediment from and deposit sediment on the bed. Experimental data were used to establish approximate similarity laws for the velocity and

concentration distribution, and to evaluate several shape factors that enter in the vertically-integrated equations of motion. Stacey and Bowen (1988) developed a simple numerical model that successfully simulated observations of small-scale, laboratory, density currents flowing down inclines of constant slope. The model results suggested that laboratory determinations of the bulk Richardson number have been biased by molecular processes but that determinations of the entrainment coefficient are probably applicable to large scale currents, and even to turbidity currents in which the gravitational driving force is provided by suspended sediment. The entrainment coefficient as a function of bottom slope is accurately simulated by the model down to slopes as small as 0.5 degree. Its value depends primarily on the stability of the current above the velocity maximum, which is not a function of the drag coefficient. Garcia (1993) conducted laboratory experiments to study the behaviour of turbidity currents in the proximity of a slope transition. Saline currents and sediment laden currents (which included two grades of silica and two grades of glass beads) were generated and the hydraulic jumps showed similar characteristics. During experiments, several velocity profiles were measured and plotted which showed a distribution resembling that of a wall jet. Altinakar et al. (1996) presented a series of experiments with turbidity currents using two different types of sediments and those experiments were supplemented by saline gravity currents. The sediments used were fine, *K-13* ($d_s = 0.047$ mm) and the coarse, *K-06* ($d_s = 0.026$ mm) sediments of specific gravity 2.65. The velocity distributions for all runs were evaluated and plotted. The turbidity current can be divided into two regions: wall region (turbulence is created by bottom shear and sediment entrainment) and jet region (turbulence is created by free shear zone and water entrainment). The height, h where the velocity is maximum, $u = U_m$ separates these regions. The velocity distribution in the wall region is expressed by logarithmic relation Eq. 2.1 or an empirical power relation Eq. 2.2 which when plotted gives an experimental value of $n = 1/6$. The distribution in the jet region is represented by a near-Gaussian relation given by Eq. 2.3. If the exponent is taken to be constant, $m = 2$, a curve fitted to the whole data set yields, $\alpha_c = 1.412 \pm 0.065$.

$$\frac{u(z)}{U_m} = \frac{1}{k} \ln z + c \quad (2.1)$$

$$\frac{u(z)}{U_m} = \left(\frac{z}{h_m} \right)^n \quad (2.2)$$

$$\frac{u(z)}{U_m} = \exp \left[-a_c \left(\frac{z - h_m}{h - h_m} \right) \right] \quad (2.3)$$

where, h and U are the height and velocity of the current.

Lee and Yu (1997) studied the hydraulic characteristics of the turbidity current in a reservoir by a series of experiments. Kaolin was used as the suspended material. The plunge points were found to be unstable initially. As the experiment went on, it moved downstream from the incipient plunge location and finally reached a stable location. The thickness of the turbidity current was found to increase while the layer-averaged velocity and concentration decrease in the longitudinal direction, the layer-averaged velocity has the smallest variation rates. Equations for the dimensionless velocity and concentration profiles were obtained. A layer with approximately constant concentration, named denser layer, was observed in the study. Sequeiros et al. (2010) presented results of a set of 74 experiments that focus on the characteristics of velocity and fractional excess density profiles of saline density and turbidity currents flowing over a mobile bed of loose granular particles. The parameters that were varied during the experiments included flow discharge, fractional excess density, bed material, and bottom slope. The profiles were plotted and analysed. Experimental data were used to establish similarity relations for vertical profiles of velocity and fractional excess density, and to evaluate shape factors used in the depth-averaged equations of motion for different flow and bed conditions.

2.3 Velocity Distribution

The velocity distribution in turbidity current in a fully developed state is almost similar to that in submerged plane wall jet. A submerged plane wall jet is described as a jet of fluid that impinges tangentially (or at an angle) on a solid wall surrounded by the same fluid (stationary or moving) progressing along the wall (Dey et al., 2010). For a turbidity current, on one side (in the inner layer), the current is confined to the bed, while on the other side (in the outer layer), it is bounded by the stationary ambient fluid (Fig. 2.1). The boundary conditions for the velocity distribution in turbidity current are such that the velocity vanishes at the bed and at the interface

between the turbidity current and the ambient fluid. Thus, the velocity distribution attains a maximum (peak velocity) at the extremity of the inner layer, that is, the junction of the inner and outer layers of the current. Below the maximum velocity level (in the inner layer), the flow is characterized by a boundary layer flow, while above the maximum velocity level (in the outer layer), the flow is structurally similar to a free jet. Therefore, the turbidity currents are composed of an inner shear layer influenced by the bed and an outer layer of the self-similar type of a shear flow (Parker et al., 1987; Stacey and Bowen, 1988; Altinakar et al., 1996).

The datasets in the form of non-dimensional stream-wise distance z/δ over non-dimensional velocity $u(z)/U_m$ are plotted and a comparison is made with the plots of Altinakar et al. (1996), Garcia (1993) and Sequeiros et al. (2010). The inner layer and outer layer of jet refer to the zones below and above the point of occurrence of maximum velocity U_m , called the jet velocity. Precisely, the jet layer ($\eta > \eta_0$) extends up to the inflection point (that is, the point of change of sign of slope (d^2u/dz^2) of a u -distribution. Below the jet layer, there exists a wall region layer ($\eta \leq \eta_0$). The jet layer thickness δ is important from the viewpoint of scaling the vertical distance z (Dey et al. 2010). η_0 refers to the ratio of z_0 (the distance from the bed where the maximum velocity occurs) to jet layer thickness δ and η refers to the ratio of z (any distance above the point of occurrence of maximum velocity) to the jet layer thickness δ .

In the near-boundary zone (that is, within the inner layer of the jet) ($\eta \leq \eta_0$), the $1/m$ -th power law is assumed which is found to fit well for the datasets.

$$\frac{u(z)}{U_m} = \frac{1}{m} \left(\frac{\eta}{\eta_0} \right)^{\frac{1}{m}} \left(1 + m - \frac{\eta}{\eta_0} \right) \quad (2.4)$$

In the jet region, $\eta > \eta_0$, boundary effects come into account and the following relation given by (Dey et al. 2010) holds well.

$$\frac{u(z)}{U_m} = \sec h^2(\eta - \eta_0) [1 + \alpha \tanh(\eta - \eta_0)] \quad (2.5)$$

where α is an additional term mainly due to submergence.

The values of m and α are calculated for all velocity profiles of experimental data and averaged. The values that gives better degree of accuracy is $m = 1/2$ and $\alpha = -1.036$ obtained by using $\eta_0 = 0.25$ and $\delta = 1$, which are contradictory to the results obtained

by Altinakar et al., (1996), i.e., $m = 1/6$ and $\alpha = 1.4$. Moreover, whether the value of m obtained is accurate or not has also been tested by power law in a different form and third-order polynomial law as,

$$\frac{u(z)}{U_m} = \zeta^{\frac{1}{m}} \quad (2.6)$$

$$\frac{u(z)}{U_m} = 1.5\zeta - 0.5\zeta^3 \quad (2.7)$$

The distance at which inflection point occurs can be obtained by equating Eq. 2.5 to zero,

$$\operatorname{sech}^2(\eta - \eta_0) [1 + \alpha \tanh(\eta - \eta_0)] = 0 \quad (2.8)$$

Putting the values of α and η_0 ,

$$1 - 1.036 \tanh(\eta - 0.25) = 0$$

$$\eta = \eta_{\max} = 2.2676 \quad (2.9)$$

The dimensionless discharge is calculated as below

$$q = \int_{\eta_0}^{\eta_1} \frac{u(z)}{U_m} d\eta + \int_0^{\eta_{\max}} \frac{u(z)}{U_m} d\eta \quad (2.10)$$

$$= \int_0^{\eta_0} \left[\frac{1\eta}{m \left(\frac{\eta}{\eta_0} \right)^{\frac{1}{m}}} \left(1 + m \frac{\eta}{\eta_0} \right) \right] d\eta + \int_{\eta_0}^{\eta_{\max}} [\operatorname{sech}^2(\eta - \eta_0) \{1 + \alpha \tanh(\eta - \eta_0)\}] d\eta$$

Solving, we get

$$q = 0.67 \quad (2.11)$$

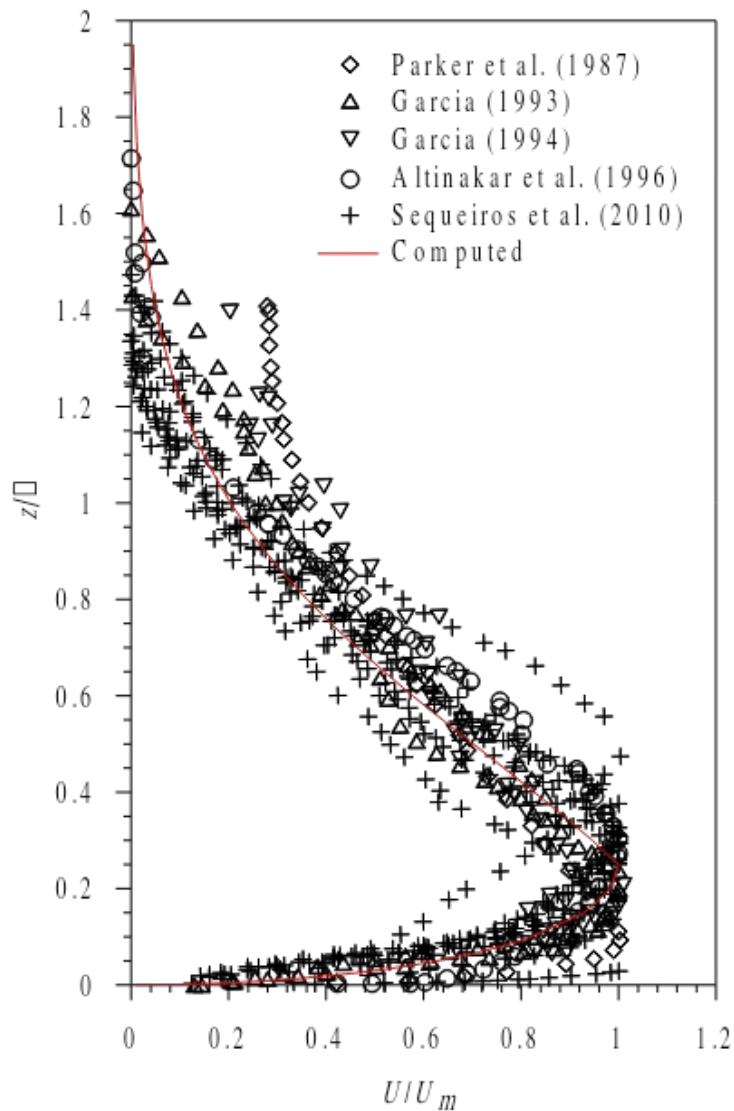


Fig. 2.2 Computed dimensionless velocity profiles

Fig. 2.2 displays the computed velocity distributions obtained from Eq. 2.4 and 2.5. The experimental data plots of turbidity and salinity currents obtained from Parker et al. (1987), García (1993,1994), Altinakar et al. (1996), Sequeiros et al. (2010) are overlapped on the computed curves in Fig. 2.2 for comparison.

2.4 Concentration distribution

The turbidity current can be considered as a self-generated current in which sediment particles are suspended by the turbulence. The transport of suspended sediment particles in turbulent flow takes place due to the advection and diffusion processes in the ambient fluid.

The concentration distribution is given:

In the near boundary zone ($\eta \leq \eta_0$), by a Rousean relation as

$$\frac{c}{C_0} = \exp\left(-w_s \int_{\eta_0}^{\eta} \frac{d\eta}{\xi_s}\right) \quad (2.12)$$

where C_0 is the reference concentration at a distance of $\eta_0 = 0.25$ from the bed where the velocity is maximum, w_s is the settling velocity of the particles and ξ_s is the diffusivity of sediment particle given as a function of η as

$$\xi_s = \beta k u_* \eta \left(1 - \frac{\eta}{\eta_0}\right)^m \quad (2.13)$$

where k is the von Kármán constant, u_* is the bed shear velocity, a coefficient $\beta = 1$ (Rouse, 1937) and m is a coefficient taken as 0.9.

Integrating Eq. 2.12 by inserting Eq. 2.13, the following expression is obtained:

$$\frac{c}{C_0} = e^{-\zeta \int \left(1 - \frac{\eta}{\eta_0}\right)^m d\eta} \quad (2.14)$$

$\zeta = w_s / \beta k u_*$ which is called the Rouse number.

In the jet region, $\eta > \eta_0$, by a Rousean relation:

$$\frac{c}{C_0} = \exp\left(-\zeta \frac{\eta - \eta_0}{\eta_{\max}}\right)^{\lambda_c} \quad (2.15)$$

$$\varepsilon_s = \beta k u_* \frac{1}{\lambda_c} (\eta - \eta_0) \left(\frac{\eta_{\max}}{\eta - \eta_0}\right)^{\lambda_c} \quad (2.16)$$

where, $\lambda_c = 0.2$ and $\zeta = 1$.

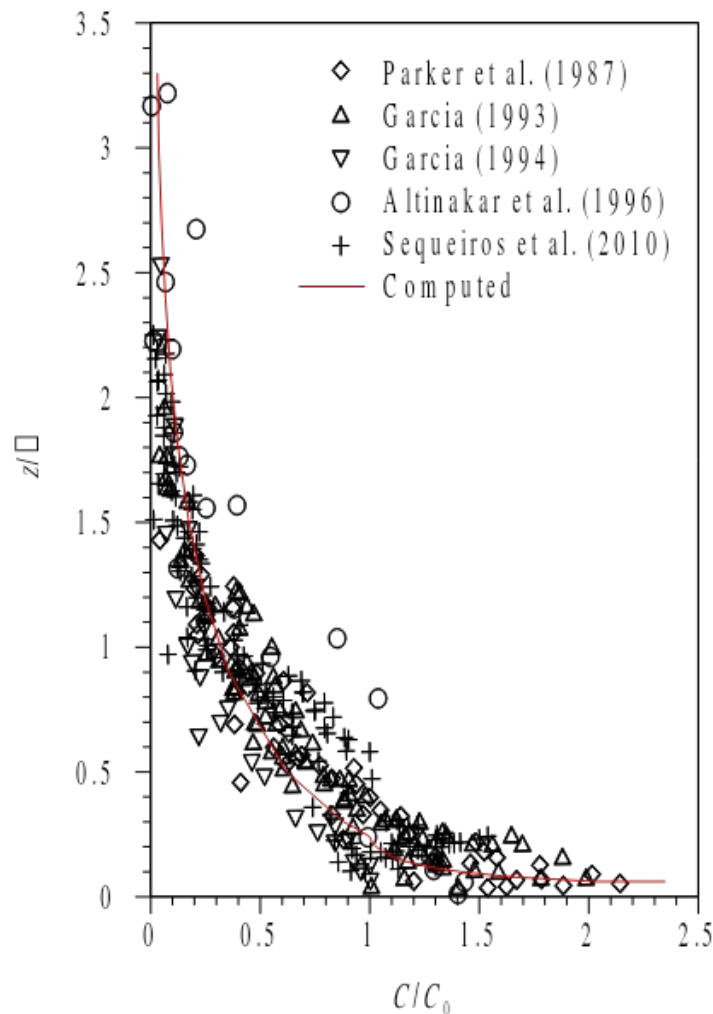


Fig. 2.3 Computed dimensionless concentration profiles

Fig. 2.3 presents the computed concentration distributions obtained from Eq. 2.14. The experimental data of Parker et al. (1987), García (1993, 1994), Altinakar et al. (1996), and Sequeiros et al. (2010) for gravity currents are shown in Fig. 2.3 for comparison.

2.5 Conclusion

The equations for velocity and concentration distributions for the near boundary and jet region are separately computed and compared with the results of previous investigators. The dimensionless profiles of velocity and of concentration are shown in Fig. 2.2 and 2.3. The modified equations gives best fit compared to the other.

References

- Akiyama, J. and Stefan, H. (1986). Turbidity current with erosion and deposition. *Journal of Hydraulic Engineering*, 111 (12), 1473–1496.
- Altinakar, M. S., Graf, W. H., and Hopfinger, E. J. (1996). Flow structure in turbidity currents. *Journal of Hydraulic Research*, 34 (5), 713–718.
- Cantero-Chinchilla, F. N., Dey, S., Castro-Orgaz, O., and Ali, S. Z. (2015). Hydrodynamic analysis of fully developed turbidity currents over plane beds based on self-preserving velocity and concentration distributions. *Journal of Geophysical Research: Earth Surface*, 120(7), 2076-2199.
- Dey, S., Nath, T. K. and Bose, S. K. (2010). Submerged wall jets subjected to injection and suction from the wall. *Journal of Fluid Mechanics*, 653, 57–97.
- Ellison, T. H. and Turner, J. S. (1959). Turbulent entrainment in stratified flows. *Journal of Fluid Mechanics*, 6 (3), 423.
- Garcia, M. H. (1993). Hydraulic jumps in sediment-driven bottom currents. *Journal of Hydraulic Engineering*, 119 (10), 1094–1117.
- Garcia, M. H. (1994). Depositional turbidity currents laden with poorly sorted sediment. *Journal of Hydraulic Engineering*, 120 (11), 1240–1263.
- Lee, H.Y. and Yu, W.S. (1997). Experimental Study of Reservoir Turbidity Current. *Journal of Hydraulic Engineering*, 123 (6), 520–528.
- Parker, G., Fukushima, Y. and Pantin, H. M. (1986). Self-accelerating turbidity currents. *Journal of Fluid Mechanics*, 171 (1), 145.
- Parker, G., Garcia, M., Fukushima, Y. and Yu, W. (1987). Experiments on turbidity currents over an erodible bed. *Journal of Hydraulic Research*, 25 (1), 123–147.
- Sequeiros, O. E., Spinewine, B., Beaubouef, R. T., Sun, T., García, M. H. and Parker, G. (2010). Characteristics of Velocity and Excess Density Profiles of Saline Underflows and Turbidity Currents Flowing over a Mobile Bed. *Journal of Hydraulic Engineering*, 136 (7), 412–433.
- Stacey, M. and Bowen, A. (1988). The vertical structure of density and turbidity currents: theory and observations. *Journal of Geophysical Research*, 93, 3528–3542.